MDPI

Article

Analysis of the Effect of the Chemical Composition of Bearing Alloys on Their Wear under Wet Friction Conditions

Marcin Madej [1],* and Beata Leszczyńska-Madej [2]

1   Faculty of Metals Engineering and Industrial Computer Science, AGH University of Krakow, 30 Mickiewicza Ave., 30-059 Krakow, Poland
2   Faculty of Non-Ferrous Metals, AGH University of Krakow, 30 Mickiewicza Ave., 30-059 Krakow, Poland; bleszcz@agh.edu.pl
*   Correspondence: mmadej@agh.edu.pl

Abstract: This paper discusses the results of a study to determine the effect of the chemical composition of two tin-based bearing alloys (B89 and B83) on their tribological properties. The tribological properties were tested using a T05 block-on-ring tester under technically dry and wet friction conditions. The research includes the determination of the wear rates, loss of mass, coefficients of friction, and changes in the coefficient of friction as a function of the process and material parameters. A study of the microstructure and base properties of such alloys, which affect the tribological properties and wear, are also presented. The study showed that chemical composition has a significant effect on the tribological properties; increasing the proportion and changing the morphology of the SnSb precipitates to rhomboidal in the B83 alloy results in an increase in wear resistance represented by loss of mass. Decreasing the size and proportion of these precipitates results in a stabilization of the frictional force variation and a slight decrease in the coefficient of friction. The research showed that SnSb phase precipitation is mainly responsible for the wear resistance of the investigated bearing alloys.

Keywords: bearing alloys; Babbitt; tribological properties; coefficient of friction; block-on-ring test

1. Introduction

A plain bearing is an important component of a mechanical system, which has found use in many industries such as the automotive, power generation, railway, and shipbuilding industries, where rolling bearings do not work. The main factors that influence the wear intensity of plain bearings are the specific load, sliding speed, temperature, movement conditions, and operating environment, in addition to the physical and mechanical properties of the friction pair materials. Many types of bearing alloys are used in industrial applications, but tin-matrix bearing alloys have the best properties for bearings with low to moderate pressures in the MPa range such as journal or linear bearings [1–3].

Tin matrix-bearing alloys typically contain around 3–8 wt% copper and 5–12 wt% antimony in their composition. The hardness, tensile strength, and fatigue strength grow with increasing copper and antimony contents in the alloy, while the ductility decreases. Alloys containing 8–12 wt% Sb and 6–10 wt% Cu in their composition show the best strength properties [4–6]. Tin Babbits are usually characterized by a three-phase microstructure. In alloys containing about 0.5–8 wt% Cu and less than 8 wt% Sb, the tin–copper intermetallic phase η (acicular precipitates of the Cu_6Sn_5 phase) and fine, rounded particles of the SbSn phase occur against a solid solution of copper and antimony in the tin (α phase). On the other hand, for an antimony content above 8 wt%, the β intermetallic phase—rhomboidal crystals of the SnSb phase—is precipitated [7,8].

Over the past 25 years, two leading trends can be distinguished in research on tin matrix bearing alloys with regard to improving the performance of these alloys, namely modification of the microstructure of bearing alloys and the design and manufacture of new composite materials based on tin Babbitts by powder metallurgy technology or by casting

methods. The authors of papers [9,10] presented results on Babbitt obtained by different coating deposition processes. The results presented in work [9] proved that both flame spraying and arc spraying are technically feasible alternatives for the application of Babbitts as they allow a favorable microstructure to be obtained with less wear under technically dry friction conditions compared to a conventionally cast alloy. The authors of paper [10] indicate that Babbitts obtained by plasma spraying have a lower wear intensity under technically dry friction conditions than a conventionally cast alloy, which is explained by the size of the β phase precipitates. In turn, Valeeva et al. [11] investigated Babbitts produced by casting and liquid forging. The results they obtained indicate a significant decrease in the wear rate of the Babbitt produced by liquid forging, which is explained by the presence of a fine grain structure in the particles of the β phase. Also, the results presented in [12] confirm that changing the morphology and size of the phases present in the Babbitt has a beneficial effect on the properties of this alloy.

Leszczyńska-Madej et al. [13,14] conducted research on the microstructure modification of tin-bearing alloys using friction stir processing (FSP). Their results demonstrated significant refinement of the microstructure of Babbits after FSP modification, which favorably affected the mechanical properties and, above all, resulted in improved wear resistance. The results of laser remelting of the surface of tin Babbits [15], as well as texturing [16], can also be found in the literature. Interesting results of Babbitt powder matrix composite coatings applied on a steel substrate were presented by Xu et al. [17]. The authors prepared a mixture consisting of Babbitt powder as the matrix material and nickel-coated graphite powders used as a self-lubricating phase, which they successively deposited by laser cladding onto a steel substrate. As a result, they obtained a good quality coating that had better wear resistance compared to a coating made of Babbitt powder alone. The results of investigations of tin-bearing alloy matrix composites can also be found in papers [18–20]. Ramadan et al. [18] produced Babbitt composite coatings on steel substrates reinforced with Al_2O_3 nanoparticles, while Ghasemi et al. [19] produced tin matrix composites reinforced with SiC and Zn particles by means of powder metallurgy technology. Stanev et al. [20] produced aluminum alloy matrix composites infiltrated with tin Babbitt. The results of studies on tin matrix composite materials are also presented in works [21,22]. Interesting results of research on composite-bearing materials can be found in work [23]. The authors investigated the dry sliding wear behavior of hybrid composites based on ZA27 alloys, reinforced with silicon carbide (SiC) and graphite (Gr). The influence of various parameters (graphite content, contact load, and sliding speed) on the wear behavior was examined using the Taguchi method. The results show that the contact load exerts the greatest influence on the specific wear rate; in contrast, the influence of the graphite content/sliding speed interaction can be neglected.

By introducing particles of reinforcing phases or by changing the morphology of the intermetallic phase precipitates in various processes, improvements in the functional properties of bearing alloys were obtained. However, the key is the chemical composition of the alloy, which influences the type and number of formed phases and thus the properties of the alloy.

Research results showing how different alloying additives, mainly Sb and Cu, affect the properties of tin matrix-bearing alloys can be found in papers [24–28], among others. Ünlü et al. [24] investigated the tribological and mechanical properties of plain bearings made of the tin alloy Sn11Sb6Cu3Pb in relation to pure metals: Sn, Pb, and Cu. The results of wear tests under wet friction conditions, using SAE-90 oil, under a load of 20 N and at a speed of 1500 rpm showed a low coefficient of friction, low bearing wear, and the lowest wear of the shaft journal made of SAE-1050 steel, for the SnSbCuPb alloy bearing, relative to those made of pure metals. On the other hand, Ishihara et al. in their paper [25] presented the results of a study on the effect of antimony in the range of 5 to 24 wt% on the wear resistance of SnSbCu alloys (the copper content was constant at 5.5 wt%). The authors reported an increase in the wear of the SnSbCu alloys for content above 18 wt% Sb. Antimony in the range of 5–18 wt% does not significantly change the wear resistance

(under liquid friction conditions); nevertheless, for contents above 20 wt% Sb, the wear resistance decreases significantly, which is explained by the loss of hard SnSb phases that accelerate frictional wear.

The authors of paper [26] noted that the wear characteristics of bearing alloys depend not only on their mechanical properties but also on their microstructure. The results presented by the authors of this work on the tribological properties under wet friction conditions showed less wear of the Sn9Sb7Cu alloy with lower hardness (40 HB) compared to the Sn20Sb16Pb3Cu alloy characterized by higher hardness (62 HB). The results of the tribological behavior of tin-based bearing alloys with different alloying contents conducted under technically dry friction conditions are presented in articles [27,28]. Zeren et al. in work [27] presented a comparison of tin Babbitts with 7 and 20 wt% Sb contents. The authors studied the effects of friction distances (up to about 1200 m), load (50–180 N), and shaft speed (200–1500 rpm) on the tribological behavior of these alloys. The results revealed less wear of the alloy with a higher antimony content, which was also characterized by higher hardness and a lower friction coefficient compared to the alloy with the lower Sb content, which was related to the presence of evenly distributed hard phases in the matrix of the alloy with about 20 wt% Sb. In addition, the authors found that both materials can be used at high shaft speeds for long periods of time without significant wear or change in bearing tolerances as the coefficient of friction rapidly decreases above 1400 rpm. Similarly, according to the authors of paper [28], the coefficients of friction determined in the scratch test were lower for the alloy with the higher Sb and Cu contents, but observations of the surface after scratching revealed a greater tendency to form microcracks in this material as the load increased, which was related to the displacement of sharp-edged SnSb phases in the soft matrix. The authors of [29] presented interesting research results for hydrodynamic steel sliding bearings with a leaded bronze lining. This sliding bearing had a reduced lifetime owing to its unequal wear. The authors compared the lining structure of this bearing with those with a high lifetime and an unused bearing. The authors proved that the reduction in bearing life was a consequence of the incorrect selection of oil. A hard and brittle layer containing Cu_3P was formed on the lining surface, resulting in increased wear.

Research centers around the world conduct studies to determine the tribological properties of various bearing materials. The tests are usually carried out on relatively short friction distances and at low loads (as a result of the pin-on-disc method), which does not fully reflect the actual operating conditions of these materials. Bearing materials with different chemical compositions and made using different methods are tested, but tin matrix-bearing alloys are still commonly used because of their very good performance properties. Two alloys were selected for testing, differing in composition to such an extent that a significant difference can be identified between the shape, size, and distribution of SnSb precipitates relevant to the properties of the bearing alloys. The present work is intended to demonstrate their prominent role in the course of friction in the typical contact of bearing alloys with steel, especially at increased countersample speeds. With the above-mentioned issues in mind, it is reasonable to conduct research on the influence of the chemical composition of bearing alloys on tribological wear under varying friction conditions (dry and wet), especially when simulating industrial conditions. The research presented in this article was conducted under technically dry friction conditions that simulate turbine start-up and under wet friction conditions using Tu-32 oil dedicated to turbine operation, at a high speed compared to the steel countersample.

2. Materials and Methods

Two grades of commercial tin-based bearing alloys, SnSb11Cu6 (B83) and SnSb8Cu4 (B89) provided the material for the study. These alloys are used for casting plain-bearing shells. The alloys were cast in cast-iron dies and then cooled in air. The chemical composition of the investigated alloys, determined using an SEM/EDS detector (Thermo Scientific NORAN System 7 X-ray microanalysis system, Thermo Fisher Scientific, Waltham, MA, USA), is shown in Table 1.

Table 1. Chemical composition of the investigated alloys, wt%.

| Name of Alloy		Chemical Composition			
Grade mark	Designation	Sn	Pb	Sb	Cu
SnSb11Cu6	B83	Rest	0.11	10.76	5.96
SnSb9Cu4	B89	Rest	0.21	7.62	3.91

The microstructure of the specimens used in this study was investigated using an OLYMPUS GX51 (LM) light microscope (Olympus, Tokyo, Japan) and a Hitachi SU 70 scanning electron microscope equipped with a thermal field emission electron gun (Schottky-type electron gun, FESEM) (Hitachi, Tokyo, Japan). Hardness measurements were performed using a Brinell hardness tester with a force of 31.25 kgf, applying a 2.5 mm diameter carbide ball according to the ASTM E10-18 standard [30]. The hardness measured was 24 ± 1.2 HB for alloy B83 and 20 ± 0.7 HB for alloy B89.

Representative results of the microstructure investigations are shown in Figures 1 and 2. The microstructure of the B83 alloy shows numerous large rhomboidal and cubic SnSb phase precipitates and numerous acicular and nearly globular Cu_6Sn_5 phase precipitates. The matrix is a solution of antimony and copper in tin (Figures 1a and 2a). The microstructure of the B89 alloy consists of a few rhomboidal precipitates of the SnSb phase and, as in the case of the B83 alloy, precipitates of the Cu_6Sn_5 phase with an acicular and nearly globular shape (Figures 1b and 2b). Detailed results of the microstructure analysis of the studied alloys are provided in the authors' earlier works [13,14].
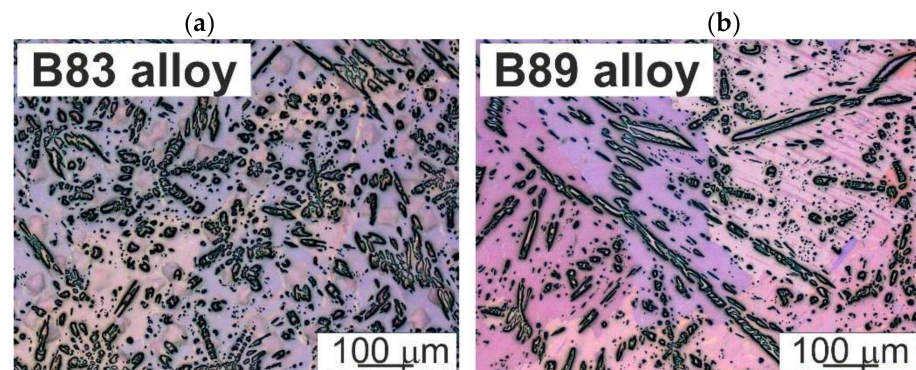

Figure 1. Microstructure of the investigated bearing alloys: (**a**) B83 alloy and (**b**) B89 alloy; light microscopy.

Tin-based bearing alloys have good lubricity, ductility, and corrosion resistance. They are characterized by good fatigue strength and abrasion resistance. They are suitable for use at high linear speeds under high loads. The tribological properties were tested using a T-05 block-on-ring tribotester (Łukasiewicz—ITeE, Radom, Poland) (Figure 3) at ambient temperature (21 °C) under technically dry and wet friction conditions. The wet sliding contact was conducted with TU-32 oil, dedicated to this type of alloy. During the test, in order to ensure proper contact between the specimen and the steel ring (heat-treated steel 100Cr6, 55 HRC, Ø49.5 × 8 mm) rotating at a constant speed, a rectangular tribological sample (4 × 4 × 20 mm) was fixed in a holder containing a hemispherical insert. The surface of the specimen in contact with the countersample was perpendicular to the direction of the load (L). A double-lever system was used to push the specimen in the direction of the ring with the accuracy of the load at ±1.5%.

Table 2 shows the friction process parameters that were used. A minimum of three tribological tests were performed for each of the materials studied.
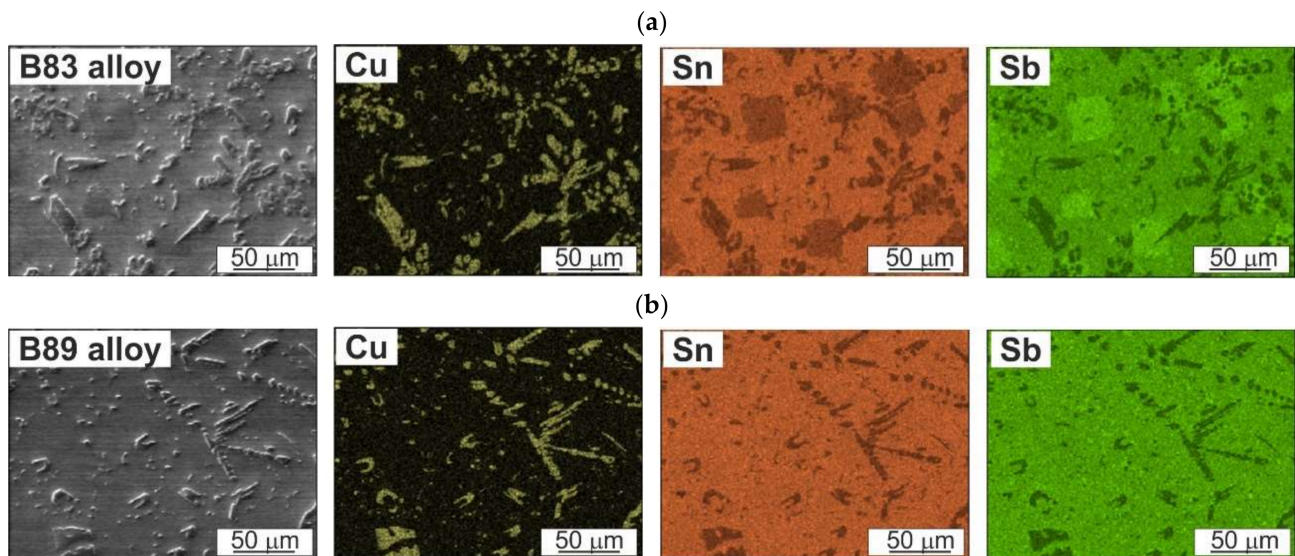
Figure 2. Microstructure and element distribution maps: Cu, Sn, and Sb; (**a**) B83 alloy and (**b**) B89 alloy; SEM.
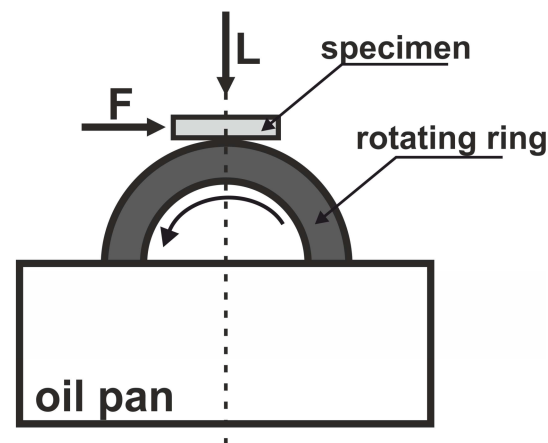
Figure 3. Diagram of the T-05 block-on-ring tribotester; F—friction force measurement and L—load perpendicular to the friction surface.

Table 2. Wear test parameters.

Sliding Contact	Countersample	Rotational Speed	Load	Sliding Distance
Technically dry	Steel 100Cr6, heat-treated, with hardness 55 HRC	200 rpm	50 N	500 m
Wet (TU-32 oil)				500 m 10,000 m

Before testing, the samples were prepared to meet specific surface quality requirements (appropriate roughness of less than 1 μm) and thoroughly degreased with a Struers degreasing agent. Following drying, the samples were weighed and tested immediately. After testing, the specimen was washed, dried, and reweighed, with the loss of mass calculated as the difference in weight. Since the initial specimens had varying weights, the loss of mass was converted into percentages to accurately assess the differences. The coefficient of friction change throughout the testing period was evaluated for the entire experiment. The load and friction force were measured to calculate the coefficient of friction. The wear surface was analyzed by a scanning electron microscope to ascertain the wear mechanisms.

3. Results and Discussion

A study was carried out to determine the effect of the Tu-32 lubricant on the friction and wear of the bearing alloy-steel 100 Cr6 friction contact at a high countersample speed of 200 rpm. The loss of mass during the test, the average coefficient of friction both wet and technically dry, and the wear rate were determined according to Equation (1):

$$w_r = \frac{\Delta m}{L \cdot Sd} \tag{1}$$

where:

Δm—loss of mass;

L—load;

Sd—sliding distance.

The following Figures 4–6 summarize the results of the loss of mass, coefficient of friction, and wear rates. The use of a lubricant, which simultaneously acts as a coolant, strongly influences the reduction in wear (Figure 4) and the wear rate (Figure 5). When comparing the two tested materials in terms of loss of mass, it can be concluded that irrespective of the friction conditions, a lower loss of mass was recorded for the B83 alloy. This is closely related to the nature of the microstructure of the alloys resulting from their chemical composition, especially the lower content of antimony and copper. The main difference is in the shape and distribution of the SnSb phases, which in B83 are large, rhomboidal in shape and relatively evenly distributed in the microstructure, in contrast to the same phases in B89, which are much smaller, fewer in number, and therefore more unevenly distributed against the tin matrix, which is responsible for the alloys' sliding properties. The second phase, which is also responsible for the increased strength properties, also differs in morphology; in B83, it has a more rounded character, in contrast to the acicular precipitates that predominate in B89 (Figures 1 and 2). These microstructural features also affect the coefficient of friction, which is summarized in Figure 6.
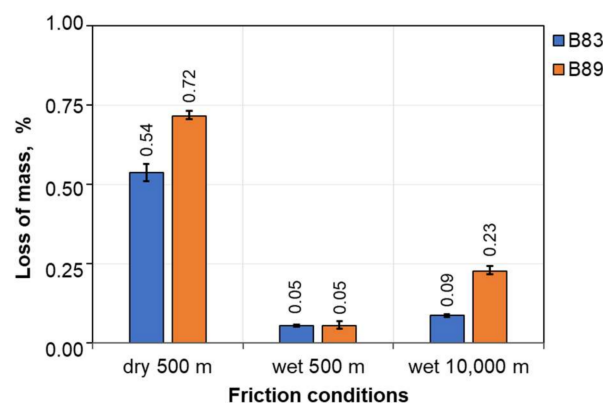
Figure 4. Effect of friction conditions and alloy type on wear resistance.

In contrast to the measured loss of mass for both alloys, the coefficient of friction resulting from the friction force measured during the test under a given load is lower for the B89 alloy (Figure 6). Hard precipitates, whose role is to improve wear resistance, slightly increase the coefficient of friction in the richer alloy and thus the proportion of SnSb and Cu_6Sn_5 phases as well. Particularly large precipitates, which strongly inhibit the removal of the matrix material, simultaneously increase the frictional force and thus the coefficient of friction under constant load as well. The coefficient of friction under wet conditions is significantly lower and within the range of coefficients recorded for wet friction pairs. In this study, a technically dry-friction test start was used, and the lubricant was supplied to the pair after half a rotation of the countersample. This is one of the reasons why the coefficient of friction decreases with the lengthening of the friction distance, as the period of stabilization of the friction conditions and the formation of a continuous lubricant film insulating the friction surfaces accounts for a smaller proportion of the total test time.
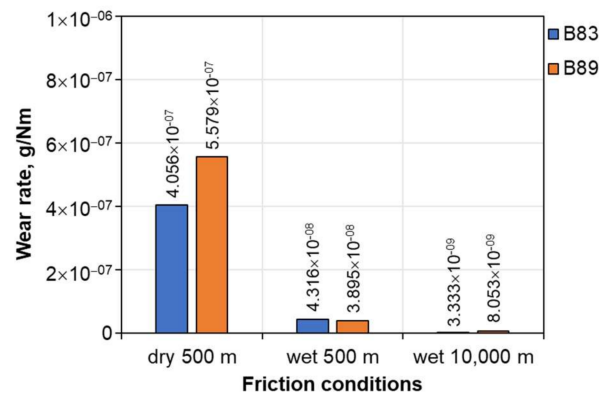
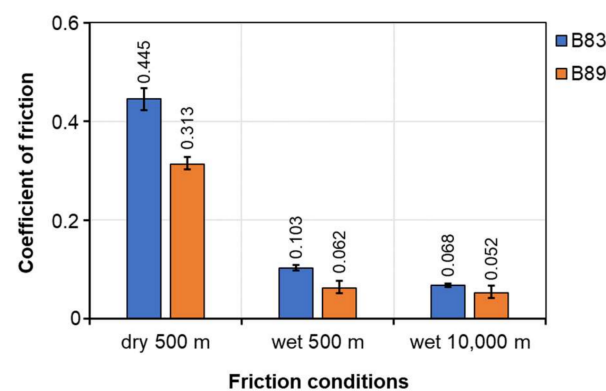**Figure 5.** Wear rate as a function of material type and friction parameters.

Figure 6. Coefficient of friction as a function of material type and friction parameters.

Plots of the friction force versus the test time were plotted at 0.5 s intervals on the basis of the recorded friction force measurements. The diagrams are shown in Figure 7. The use of Tu 32 oil stabilized the friction force curve for both of the investigated alloys. Under both wet and dry conditions, the friction force during the test for B83 is higher than that for the B89 alloy. In the dry test, the force variation also has a more "stable" character for the B89 alloy, in contrast to the force variation for the B83 alloy, which is highly unstable with numerous spikes. This is due to the interaction of the numerous precipitates of SnSb and Cu_6Sn_5 phases in the friction pair, temporarily blocking the smearing of the tin matrix over the surface and interacting with the fine $Cr_{23}C_6$ carbides protruding from the surface of the countersample, which can lead to their cracking and consequent chipping. All of these phenomena can influence the abrupt changes in the friction force seen in Figure 7. Alloy B89 is characterized by a much more stable course of frictional force, with few abrupt changes and a much smaller range of magnitude than alloy B83 owing to the morphology and distribution of hard phases, especially SnSb. The run-in time of the researched alloys is very short; for B83, it is 25 s, and for B89, it is only 15 s. This is the result of their properties and the corresponding surface preparation used in both research and industrial bearings. Under wet friction conditions with a dry start, the contact time varies; with B83 at about 1000 s and B89 at about 3500–4500 s, depending on the test, the decrease in frictional force is smoother due to the nature of the microstructure of this alloy, and the differences in individual tests may result from slight variations in the roughness of the surfaces prepared for testing. The influence of the environment on the results can be eliminated since the tests were conducted under constant conditions, in a room with a temperature of 21 °C and humidity of 40 ÷ 45%. Relating the wear resistance results obtained in the present study to tests carried out at a rotational speed of 136 rpm under the same conditions, it can be seen that increasing the speed to 200 rpm results in an almost three-fold increase in wear in the B89 alloy over a distance of 10,000 m [31] and a two-fold increase in the B83 alloy. This is the result of a change in frictional dynamics, a small but, for the tin matrix, significant

increase in temperature at the friction pair. These increased values of loss of mass do not correspond to an increase in the coefficients of friction, which in alloy B89 is almost halved with increasing rotation, and in alloy B83, it is similar.

(**a**) (**b**)
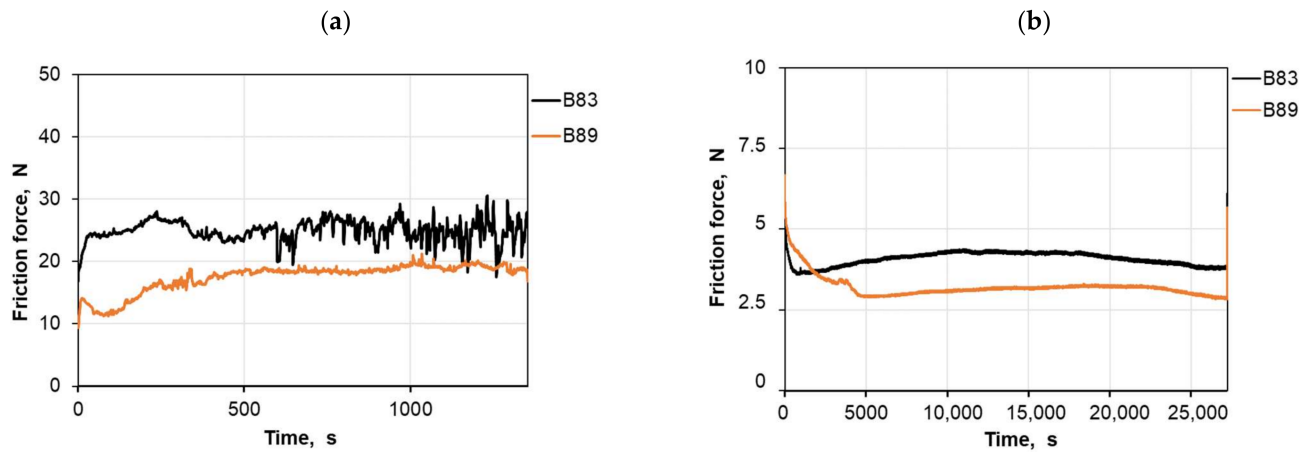
Figure 7. Friction force of investigated alloys as a function of time and processing conditions; (**a**) technically dry friction, sliding distance of 500 m, and (**b**) lubricated friction, sliding distance of 10,000 m.

Wear Mechanisms

In addition to determining the basic properties of the material under the applied tribological test conditions, it is very important to identify the phenomena occurring at the friction pair, which can be identified by observing the surface morphology after friction. This allows the friction mechanisms that occurred during the test to be identified. Figures 8–15 presented below summarize typical examples of the post-friction surface morphology of the studied alloys.
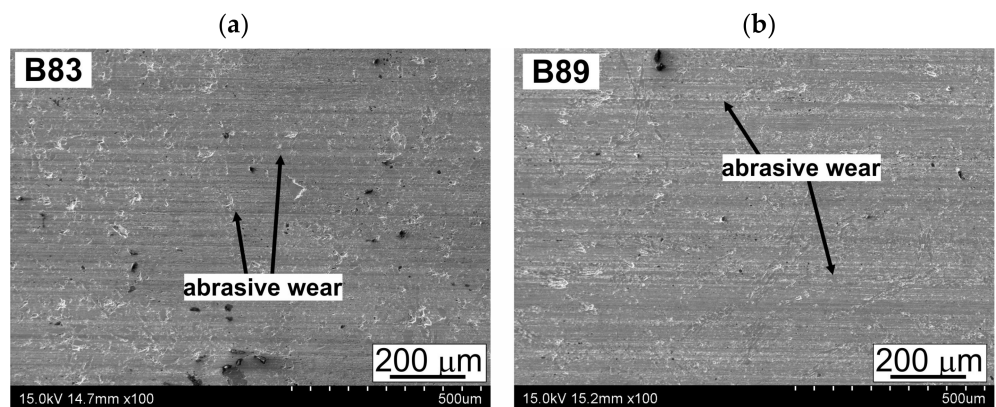
(**a**) (**b**)
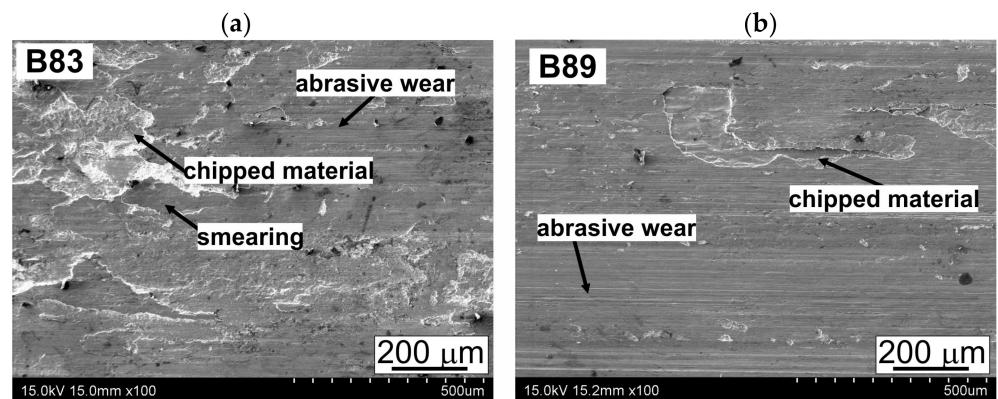
Figure 8. Surface morphology after sliding contact under technically dry friction: (**a**) B83 alloy and (**b**) B89 alloy; SEM.
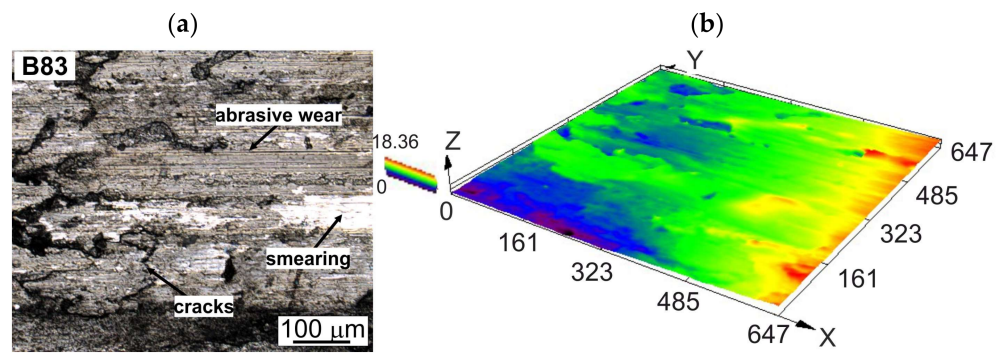
Figure 9. Surface morphology of the B83 alloy after sliding contact under technically dry friction: (**a**) 2D view and (**b**) 3D view; confocal microscopy.
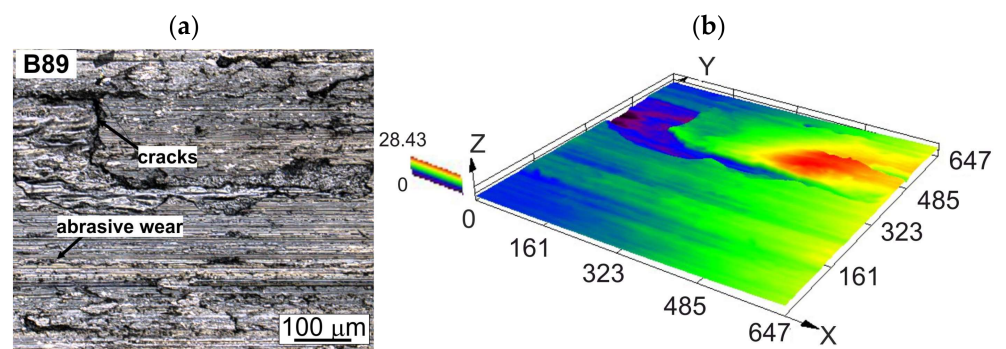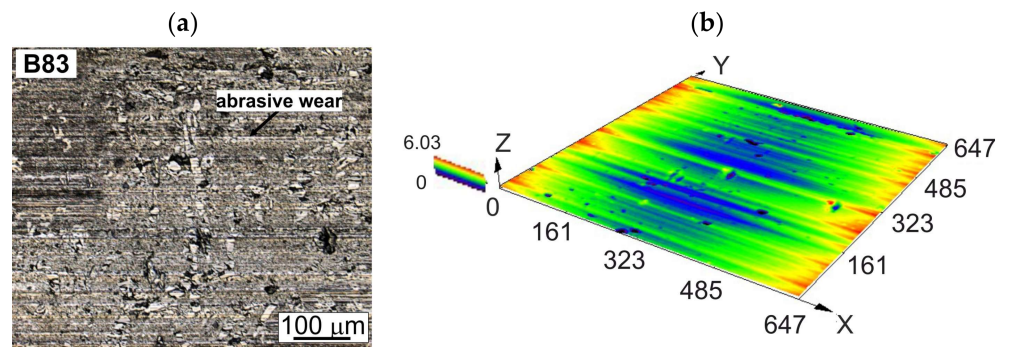

Figure 10. Surface morphology of the B89 alloy after sliding contact under technically dry friction: (**a**) 2D view and (**b**) 3D view; confocal microscopy.
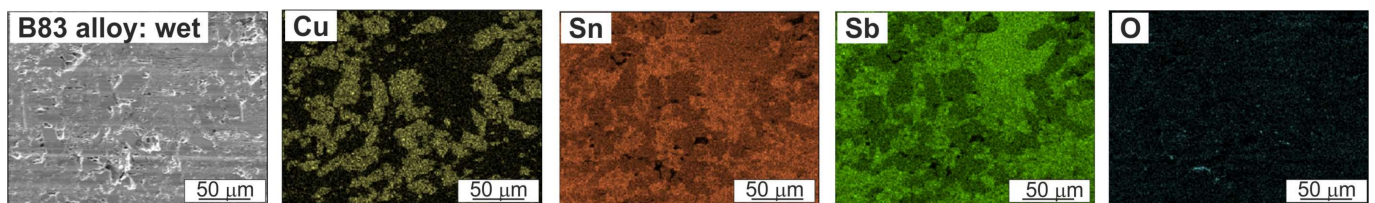

Figure 11. Surface morphology after sliding contact under the condition of wet friction: (**a**) B83 alloy and (**b**) B89 alloy; SEM.
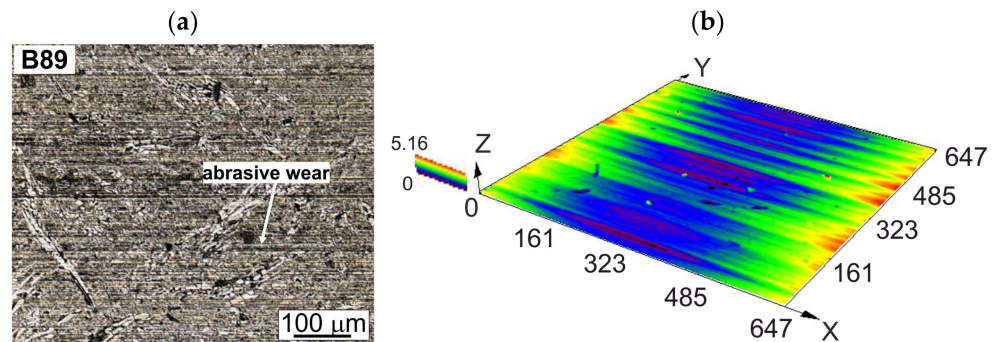
Figure 12. Surface morphology of the B83 alloy after sliding contact under the condition of wet friction at a distance of 10,000 m: (**a**) 2D view and (**b**) 3D view; confocal microscopy.

Figure 13. Element distribution maps (Cu, Sn, Sb, and O) on the surface of the B83 alloy after friction under wet conditions at a distance of 10,000 m; SEM.

Figure 14. Surface morphology of the B89 alloy after sliding contact under wet friction at a distance of 10,000 m: (**a**) 2D view and (**b**) 3D view; confocal microscopy.
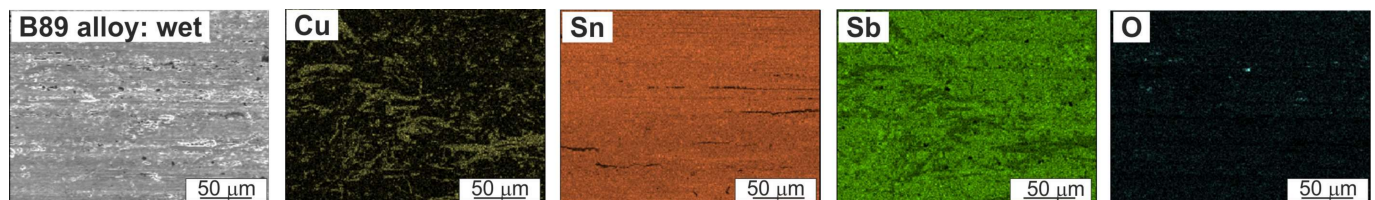
Figure 15. Element distribution maps (Cu, Sn, Sb, and O) on the surface of the B89 alloy after friction under wet conditions at a distance of 10,000 m; SEM.

Typical examples of the friction surfaces of both alloys tested under dry friction conditions, shown in Figure 8, allow us to conclude that the dominant wear mechanism in the investigated alloys is abrasive wear, consisting of scratching and furrowing of the surfaces of the studied materials. The domination of these mechanisms is because of both the nature of the surface of the countersample made of 100 Cr6 steel, with it having protruding carbides of the $Cr_{23}C_6$ type on its surface, which are much harder than the studied two alloys, and the possible chipping of SnSb and Cu_6Sn_5 phases can act as an abrasive in the friction pair for some time. The presence of an abrasive significantly

intensifies the wear processes, so it becomes important to design the pair in such a way that such particles of higher hardness can be quickly removed from at least one of the materials involved in friction. The surface analysis also indicates that local plastic displacement of the matrix material can be observed, resulting in the formation of cavities. A detailed surface analysis was performed using a confocal microscope, and the following Figures 9 and 10 display the results of these analyses.

The friction surface analysis of the B83 alloy presented in Figure 9 shows that in addition to abrasive mechanisms, transverse cracking as well as transfer and smearing are observed along the surface of the matrix material. The movement of the matrix over the surface is inhibited by the precipitates of large rhomboidal or hexagonal SnSb particles. In the B89 alloy, we can also observe smearing of the matrix material, cracking both transversely and parallel to the friction direction (Figure 10). The 3D analysis indicates that in this alloy, the lack of large SnSb particles inhibiting tin displacement in alloy B83 does not result in localized areas of tin smearing. The finer and evenly distributed Cu_6Sn_5 precipitates do not prevent tin movement across the surface either. Therefore, large and clearly visible areas of tin smearing are not observed in alloy B89 as in alloy B83 (Figure 9a). Despite this phenomenon, the course of the friction force change as a function of time is still clearly more stable compared to alloy B83. On the surface of both alloys, areas of film build-up can be seen, which may indicate the presence of a wear mechanism involving oxidation.

A technically dry friction test was carried out to determine the tribological properties of the researched alloys in the event of failure of the oil supply system to the bearing and to compare the performance of the materials under technically dry and wet conditions. Surface morphology observations after sliding contact were also made after the wet tribological test, typical examples of which are summarized in Figures 11–15 presented below.

The use of a lubricant in the form of Tu-32 oil changes the nature of the surface after sliding contact, eliminating all mechanisms associated with material displacement, especially the tin matrix. The surface observed using a scanning microscope is characterized by the presence of fine scratches that indicate the presence of an abrasive in the oil, which may be due to the limited volume of the reservoir from which the countersample draws oil to the friction pair, facilitating the accumulation of hard particles in suspension that may have been chipped off in the initial stage of dry friction. Both surfaces have a similar character, with the alloy surface showing a higher number of fine precipitates owing to the nature of the microstructure, while the B83 alloy shows large SnSb precipitates at this stage of friction since no build-up of matrix material can be seen on them (Figures 11 and 13). Surface studies of the sliding contact after wet friction were also performed using a confocal microscope to analyze the friction processes in more detail. The results of the observations are summarized below and presented in Figures 12 and 14 and supplemented by the results of the friction surface chemical analysis study presented in the form of element distribution maps (Figures 13 and 15). The wear mechanisms identified in the investigated alloys compared to the same alloys tested at 136 rpm are convergent [31]; no mechanisms are observed that would indicate significant surface degradation along the same friction path at an increased rpm despite a significant rise in loss of mass in the B89 alloy. This is confirmed by the areas of oxygen visible in the elemental distribution maps (Figures 13 and 15) and the high affinity of copper and tin for oxygen, which are the alloying elements according to the Richardson–Ellingham diagram.

The analyses of the surface morphology after sliding contact at a rotational countersample speed of 200 rpm presented in the above Figures 11–15 show that the use of Tu-32 oil reduces friction only to abrasive mechanisms, and as the 3D analyses show, this is mainly in the form of micro-scratching, but the depth of these scratches is very slight. Careful analysis of the friction surface of the B83 alloy shows that cracks are also visible within the large SnSb precipitates, probably resulting from contact with the protruding $Cr_{23}C_6$ carbides on the surface of the countersample and characterized by the significantly higher hardness than the SnSb particles. Small areas of deposition of the tin matrix can

also be distinguished on their surface; such phenomena are not observed on the surface of the B89 alloy. These tin lumps change the surface of the tin matrix; we observe areas with characteristics similar to those of the adhesion mechanism; nonetheless, they are more a consequence of the plastic deformation associated with the ductility and low hardness of the tin. An examination of the chemical composition of the area of the surface involved in friction showed that oxides, which are copper and tin oxides, are also observed locally, but there are far fewer of them than in the case of dry friction. Research also confirmed that no transfer of iron or other elements from 100Cr6 steel (the countersample) to the surface of the alloys was observed. This indicates that the oil used properly insulates the friction surfaces and has a cooling function in the friction pair, preventing thermal interaction and thus diffusion. The influence of the SnSb precipitates is confirmed by the distribution of Sb on the surface after friction: in B83, it is unevenly distributed, with lower concentrations observed mainly in the built-up areas of the tin matrix, while in B89 it is relatively evenly distributed, confirming the ease with which the matrix smears and very fine SnSb precipitates move across the surface during friction; thus, a lower coefficient of friction was measured and a stable course of frictional force variation as a function of tribological test time was observed. The research confirmed the significant role of the correct shape and distribution of the SnSb precipitates in friction processes. A comparison of the two alloys differing in their shape and distribution confirmed this fact, which was partly reported in the work of Valeeva, A.K. et al. [11], where one particular alloy composition with these precipitates was studied.

4. Conclusions

Comparative tests were carried out on two bearing alloys that differed in their chemical composition, namely B83 and B89. A high-speed countersample was also used in the test, which was carried out under both technically dry and wet friction conditions. The obtained results allowed the following conclusions to be drawn:

- The investigated alloys differ in microstructure, mainly owing to the distribution and shape of the SnSb precipitates, which are large and rhomboidal in alloy B83 and small and unevenly distributed in alloy B89. This also translates into the hardness of the tested alloy, which is 24 HB for alloy B83 and 20HB for alloy B89.
- These microstructure characteristics result in lower technically dry and wet friction losses of mass in the studied B83 alloy, resulting in higher wear resistance and lower wear rates.
- The coefficient of friction for the alloys tested under wet and technically dry friction conditions is higher for the B83 alloy, which is also because of the microstructural characteristics of the investigated alloys, in which the tin matrix is more important in alloy B89.
- Alloy B83, with its increased copper and antimony content, is characterized by better wear resistance and less susceptibility to increased rotation of the interacting parts.
- SnSb-type precipitates were observed to be a major factor influencing friction, mainly by regulating the smearing of the tin matrix across the surface after tribological contact.

Author Contributions: Conceptualization, M.M. and B.L.-M.; methodology, M.M. and B.L.-M.; formal analysis, M.M. and B.L.-M.; investigation, M.M. and B.L.-M.; writing, M.M. and B.L.-M.; writing—review and editing, M.M. and B.L.-M.; visualization, M.M. and B.L.-M. All authors have read and agreed to the published version of the manuscript.

Institutional Review Board Statement: Not applicable.

Informed Consent Statement: Not applicable.

Data Availability Statement: Not applicable.

Conflicts of Interest: The authors declare no conflict of interest.

References

1. Pratt, G.C. Materials for Plain Bearings. *Int. Metall. Rev.* **1973**, *18*, 62–88. [CrossRef]
2. Babu, M.V.S.; Krishna, A.R.; Suman, K.N.S. Review of Journal Bearing Materials and Current Trends. *Am. J. Mater. Sci. Technol.* **2015**, *4*, 72–83. [CrossRef]
3. Mironov, A.; Gershman, I.; Gershman, E.; Podrabinnik, P.; Kuznetsova, E.; Peretyagin, P.; Peretyagin, N. Properties of Journal Bearing Materials That Determine Their Wear Resistance on the Example of Aluminum-Based Alloys. *Materials* **2021**, *14*, 535. [CrossRef] [PubMed]
4. *ASTM B23-00*; Standard Specification for White Metal Bearing Alloys (Known Commercially as "BabbittMetal"). ASTM International: West Conshohocken, PA, USA, 2014.
5. Leszczyńska-Madej, B.; Madej, M.; Hrabia-Wiśnios, J. Effect of chemical composition on the microstructure and tribological properties of Sn-based alloys. *J. Mater. Eng. Perform.* **2019**, *28*, 4065–4073. [CrossRef]
6. Sadykov, F.A.; Barykin, N.P.; Valeev, I.S.; Danilenko, V.N. Influence of the structural state on mechanical behavior of tin babbit. *J. Mater. Eng. Perform.* **2003**, *12*, 29–36. [CrossRef]
7. Goudarzi Moazami, M.; Jenabali Jahromi, S.A.; Nazarboland, A. Investigation of characteristics of tin-based white metals as a bearing material. *Mater. Des.* **2009**, *30*, 2283–2288. [CrossRef]
8. Barry, B.T.; Thwaites, C.J. *Tin and Its Alloys and Compounds*; Ellis Horwood Ltd Publisher: Herts, UK; University Michigan: Ann Arbor, MI, USA, 1983.
9. Campos Alcover, P.R., Jr.; Marenda Pukasiewicz, A.G. Evaluation of microstructure, mechanical and tribological properties of a Babbitt alloy deposited by arc and flame spray processes. *Tribol. Int.* **2019**, *131*, 148–157. [CrossRef]
10. Barykin, N.P.; Sadykov, F.A.; Aslanyan, I.R. Wear and failure of babbit bushes in steam turbine sliding bearings. *J. Mater. Eng. Perform.* **2000**, *9*, 110–115. [CrossRef]
11. Valeeva, A.K.; Valeev, I.S.; Fazlyakhmetov, R.F. On the Wear Rate of an $Sn_{11}Sb_{5.5}Cu$ Babbitt. *J. Frict. Wear.* **2017**, *38*, 53–57. [CrossRef]
12. Potekhin, B.A.; Il'yushin, V.V.; Khristolyubov, A.S. Effect of casting methods on the structure and properties of tin babbit. *Met. Sci. Heat. Treat.* **2009**, *51*, 378–382. [CrossRef]
13. Leszczyńska-Madej, B.; Madej, M.; Hrabia-Wiśnios, J.; Węglowska, A. Effects of the Processing Parameters of Friction Stir Processing on the Microstructure, Hardness and Tribological Properties of SnSbCu Bearing Alloy. *Materials* **2020**, *13*, 5826. [CrossRef] [PubMed]
14. Leszczyńska-Madej, B.; Hrabia-Wiśnios, J.; Węglowska, A.; Perek-Nowak, M.; Madej, M. Experimental investigations of heat generation and microstructure evolution during friction stir processing of SnSbCu alloy. *Archiv. Civ. Mech. Eng.* **2022**, *22*, 202. [CrossRef]
15. Dong, Y.N.; Tong, Z.; Li, X.; Wang, W. Effect of laser remelting on tribological properties of Babbitt alloy. *Mater. Res. Express* **2019**, *6*, 096570. [CrossRef]
16. Zhang, H.; Zhang, D.Y.; Hua, M.; Dong, G.N.; Chin, K.S. A Study on the Tribological Behavior of Surface Texturing on Babbitt Alloy under Mixed or Starved Lubrication. *Tribol. Lett.* **2014**, *56*, 305–315. [CrossRef]
17. Xu, T.Z.; Zhang, S.; Wang, Z.Y.; Zhang, C.H.; Zhang, D.X.; Wang, M.; Wu, C.L. Wear behavior of graphite self-lubricating Babbitt alloy composite coating on 20 steel prepared by laser cladding. *Eng. Fail. Anal.* **2022**, *441*, 106698. [CrossRef]
18. Ramadan, M.; Alghamdi, A.S.; Subhani, T.; Halim, K.S.A. Fabrication and Characterization of Sn-Based Babbitt Alloy Nanocomposite Reinforced with Al_2O_3 Nanoparticles/Carbon Steel Bimetallic Material. *Materials* **2020**, *13*, 2759. [CrossRef] [PubMed]
19. Ghasemi, F.; Moazami-Goudarzi, M.; Najafi, H. Microstructures, hardening and tribological behaviors of tin matrix composites reinforced with SiC and Zn particles. *Rare Met.* **2021**, *40*, 2584–2592. [CrossRef]
20. Stanev, L.; Kolev, M.; Drenchev, L.; Boyko, K. Fabrication Technique and Characterization of Aluminum Alloy-Based Porous Composite Infiltrated with Babbitt Alloy. *J. Mater. Eng. Perform.* **2020**, *29*, 3767–3773. [CrossRef]
21. Kolmakov, A.G.; Kalashnikov, I.E.; Bolotova, L.K.; Podymovab, N.B.; Bykova, P.A.; Katina, I.V.; Kobelevaa, L.I. Study of Characteristics of Composite Materials Based on B83 Antifriction Alloy. *Inorg. Mater.* **2020**, *56*, 1499–1505. [CrossRef]
22. Rajkumar, S.G.; Navthar, R.R. Tribological Investigation and Development of Tin Based Babbit Composite Material. *Int. Res. J. Eng. Technol.* **2017**, *4*, 3190–3196.
23. Miloradović, N.; Vujanac, R.; Stojanović, B.; Pavlović, A. Dry sliding wear behaviour of ZA27/SiC/Gr hybrid composites with Taguchi optimization. *Compos. Struct.* **2021**, *264*, 113658. [CrossRef]
24. Ünlü, B.S. Determination of the tribological and mechanical properties of SnPbCuSb (white metal) bearings. *Mater. Sci.* **2011**, *46*, 478–485. [CrossRef]
25. Ishihara, S.; Kiyoshi, T.; Takahito, G. Effect of amount of antimony on sliding wear resistance of white metal. *Tribol. Int.* **2010**, *43*, 935–938. [CrossRef]
26. Feyzullahoglu, E.; Zeren, A.; Zeren, M. Tribological behaviour of tin-based materials and brass in oil lubricated conditions. *Mater. Des.* **2008**, *29*, 714–720. [CrossRef]
27. Zeren, A.; Feyzullahoglu, E.; Zeren, M. A study on tribological behaviour of tin-based bearing material in dry sliding. *Mater. Des.* **2007**, *28*, 318–323. [CrossRef]
28. Ozgur, B.M.; Coban, O.; Sinmazcelik, T.; Gunay, V.; Zeren, M. Instrumented indentation and scratch testing evaluation of tribological properties of tin-based bearing materials. *Mater. Des.* **2010**, *31*, 2707–2715. [CrossRef]

29. Luštinec, J.; Očenášek, V.; Kec, J. Damage of the CuPb20 sliding bearing. *Appl. Eng. Lett.* **2017**, *2*, 16–21.
30. *ASTM E10-18*; Standard Test Method for Brinell Hardness of Metallic Materials. ASTM International: West Conshohocken, PA, USA, 2017.
31. Madej, M.; Leszczyńska-Madej, B.; Hrabia-Wiśnios, J.; Węglowska, A. Effect of FSP on Tribological Properties of Grade B89 Tin Babbitt. *Materials* **2021**, *14*, 2627. [CrossRef]